

Calculations on fission gas behaviour in the high burnup structure

P. Blair ^{a,b,*}, A. Romano ^a, Ch. Hellwig ^a, R. Chawla ^{a,b}

^a Paul Scherrer Institut, CH 5232 Villigen-PSI, Switzerland

^b Ecole Polytechnique Fédérale de Lausanne (EPFL), CH-1015, Lausanne, Switzerland

Received 5 October 2005; accepted 30 January 2006

Abstract

The behaviour of fission gas in high burnup fuel during steady-state and transient conditions is of special interest for safety reasons. Despite this, mechanistic models that reflect the fission gas transport processes and reliably predict the evolution of the remaining fission gas in the high burnup structure (HBS) are largely missing today. We start to address this problem by developing a one-dimensional, mass balance model and apply it to LWR UO₂ fuel at the moderate temperatures found in the rim region. We examine the quantity of gas remaining in the HBS fuel matrix at steady state and compare it with experimental values. We find that the current model reproduces the 0.2 wt% observed xenon concentration under certain conditions, viz. fast grain boundary diffusion and an effective volume diffusion coefficient. A sensitivity analysis is also conducted for the model parameters, the relative importance for which is not well established a priori.

© 2006 Elsevier B.V. All rights reserved.

PACS: 28.41.Ak; 66.30.–h

1. Introduction

Nuclear fuel has seen intensive development during recent years because of the economic potential of achieving high discharge burnups in nuclear reactors [1]. As a consequence of these burnup increases the in-pile behaviour of the so-called high burnup structure (HBS) [2–14] is of great interest. There are still a number of open questions regarding the formation and fuel performance of the HBS. In

particular the fission gas behaviour under transient conditions is of special interest for safety reasons. The fission gas transport processes during steady state irradiation are important in this context as the location and quantity of the remaining fission gas in the high burnup structure is necessary as an input for modeling the fuel performance during design basis accidents, e.g. reactivity-initiated accidents (RIA) and loss-of-coolant accidents (LOCA) [2–4]. However, whilst the fission gas behaviour in fuel for moderate burnups is well characterised and the main processes are reflected in many models [15–18], fission gas behaviour in high burnup fuel is still a matter of research. A few models have been developed [5,6] and there has been a comprehensive

* Corresponding author. Address: Paul Scherrer Institut, CH 5232 Villigen-PSI, Switzerland. Tel.: +41 56 310 2285; fax: +41 56 310 2203.

E-mail address: paul.blair@psi.ch (P. Blair).

characterization of the HBS, e.g. the associated xenon depletion [7–12]. Despite this, mechanistic models that reflect the fission gas transport processes and reliably predict the evolution of the remaining fission gas in high burnup fuel are scarce.

We have addressed this problem by developing a one-dimensional, mass balance model. In this paper, the model is presented and is applied to LWR UO₂ fuel at the moderate temperatures found in the rim region. As a first validation step, we examine the quantity of gas remaining in the HBS fuel matrix at steady state and compare it with experimental values. The model contains several parameters for which the relative importance is not well established a priori and so a sensitivity analysis is conducted in order to clarify this aspect. Throughout this study the calculated averaged xenon concentration is used for comparison with the concentration measurements made by electron micro-probe analysis (EPMA) of high burnup fuel. For the high burnup structure the measured xenon depletion is typically ~0.2 wt% [8] and it is with respect to this value that we compare the results from the calculations.

The next section describes the model structure, assumptions made and the adopted mathematical formulation. Results are presented and discussed in Section 3.

2. Fission gas model

Fission gas release models for low to moderate burnups typically consider three basic processes: volume diffusion within the fuel matrix including the precipitation of single atoms into intra-granular bubbles [19], precipitation and growth (and shrinkage/destruction) of grain boundary gas bubbles and inter-linkage of grain boundary bubbles resulting in release to the pin free volume. Within each of these processes there are usually several different sub-processes acting on different phases of the gas, e.g. irradiation induced resolution that affects the shrinkage of grain boundary gas bubbles. For most fission gas release models, up to four separate phases are considered in calculating the distribution of gas within the normal fuel structure, i.e. gas within the matrix, gas trapped in intra-granular bubbles, gas trapped within grain boundary bubbles and grain boundary gas that is free to diffuse (the last two comprising the grain boundary phases).

The model presented here includes the first two processes indicated above with the principal addition of grain boundary diffusion. In fact, while in

the normal fuel structure at medium burnups grain boundary diffusion is not significant [20], in the HBS the increase in the grain boundary density due to the reduced grain size distribution, the absence of important grain boundary porosity and the decrease in the average pore to pore separation enhance the importance of the grain boundary transport mechanisms.

The model also includes the effect of irradiation induced resolution within the two grain boundary gas phases. The resolution process occurs when a fission fragment passes near a bubble (intra or inter-granular). It is well established that if the bubble is small enough the high local temperatures can completely destroy the bubble. For this reason a stable population of nm-sized intra-granular bubbles exists in the normal fuel structure from early on in the irradiation [19]. However, for larger grain boundary bubbles this does not occur and instead a ‘chipping’ model is usually employed in which a proportion of the gas is removed without complete bubble destruction [20,21].

We introduce a one-dimensional chain of nodes, with a nodal separation equal to a grain diameter (~300 nm), lying between two HBS pores, which act as perfect gas sinks. At each node there are three gas phases: gas inside the fuel volume, gas which is free to move on the grain boundaries and gas which is trapped in grain boundary bubbles (and is therefore immobile). For each of these phases various transport processes are considered, which move the gas from one phase to another: lattice diffusion of the matrix gas, irradiation induced resolution of grain boundary gas, trapping and grain boundary diffusion of the free grain boundary gas. These processes combine to form the following set of mass balances for each phase of gas at each node

$$J_{so} + J_{re}^{fr} + J_{re}^{tr} - J_{di}^{fr} - J_{di}^{tr} = 0, \tag{1}$$

$$J_{di}^{fr} - J_{re}^{fr} - J_{tr}^{fr} - J_{di}^{gb} = 0, \tag{2}$$

$$J_{di}^{tr} - J_{re}^{tr} + J_{tr}^{tr} = 0, \tag{3}$$

where the J terms are mass fluxes in units of s⁻¹ and are defined as

J_{so}	production rate of xenon
J_{re}^{fr}	resolution rate from the free gas phase of the grain boundary to the bulk volume gas phase
J_{re}^{tr}	resolution rate from the trapped gas phase of the grain boundary to the bulk volume gas phase

$J_{\text{di}}^{\text{fr}}$	rate of gas transfer from the grain phase to the free phase via a diffusive process
$J_{\text{di}}^{\text{tr}}$	rate of gas transfer from the grain phase to the trapped phase via a diffusive process
$J_{\text{tr}}^{\text{fr}}$	rate of trapping from the free grain boundary phase to the trapped phase
$J_{\text{di}}^{\text{gb}}$	rate of gas transfer for the free gas phase via the grain boundary diffusion process

Each of the rate terms, with the exception of the xenon production rate, is a function of the local gas concentration. The xenon production rate can be written as

$$J_{\text{so}} = \dot{F} Y_{\text{Xe}} V_v, \quad (4)$$

where \dot{F} is the local fission rate density, Y_{Xe} is the stable Xe chain yield and V_v is the volume of the matrix associated with the node in question (the volume of a single spherical grain is used here). The local fission rate density is calculated using a pellet (radially) averaged fission rate density and a power peaking factor for the rim zone.

The resolution terms for the trapped and free gas phases and the rate of trapping of the free phase are calculated using the formulation of Van Uffelen [22], i.e.

$$J_{\text{re}}^k = \Gamma_{\text{re}}^* \frac{\dot{F}}{\dot{F}_{\text{ref}}} C_k(i) V_k, \quad (5)$$

$$J_{\text{tr}}^{\text{fr}} = \Omega C_{\text{fr}}(i) V_k, \quad (6)$$

where $C_k(i)$ is the local gas concentration (m^{-3}) at node i for either the free or trapped phases, V_k is the volume associated with the concentration $C_k(i)$ and Γ_{re}^* is the reference resolution rate coefficient at the fission rate density \dot{F}_{ref} . This reference fission rate density is usually calculated for a local linear heat rate of 20 kW/m. The parameter Ω is the trapping rate coefficient and is a function of several variables e.g. bubble number density and radius [22]. Finally the diffusive rates for both the volume and grain boundary diffusion are calculated using Fick's law and the respective local concentrations, surface areas and diffusion coefficients. This applies to both the bulk and grain boundary diffusion processes.

In addition to these processes there are six principal assumptions:

1. The grain boundary bubbles are in a nucleation phase and do not undergo significant growth.
2. The large HBS pores form perfect sinks for the diffusing fission gas.

3. The system is studied under steady-state conditions.
4. The study only considers xenon gas because the available EPMA measurements primarily refer to xenon.
5. The volume diffusion coefficient is calculated using the correlation from Kogai [17].
6. The grain boundary diffusion coefficient is calculated as a multiple of the volume diffusion coefficient. A diffusion coefficient ratio $\alpha = D_{\text{gb}}/D_v$ is thus introduced as in [23] ranging from 10^2 to 10^6 .

In normal fuel structure, assumption 1 would be considered unrealistic, however there have been some observations of nm-sized grain boundary bubbles in high burnup fuel [12] that would seem to indicate a lack of growth of grain boundary fission gas precipitates. In spite of this, we introduce a bubble growth process that assumes equilibrium between the bubble pressure and the surface tension and calculates the radius required to satisfy this condition as a function of the amount of gas in the bubble. This allows assessment of the validity of this assumption in the context of the model. This condition is considered throughout the solution of the main equations. It should also be noted that as a consequence of assumption 3, the flux of gas to the pores (the primary sinks) must be equal to the total production of gas in the system to maintain a mass balance.

The solution to the system of Eqs. (1)–(3) at each node gives a detailed profile of the gas concentrations between the pores for each of the three fission gas phases. However the HBS concentrations measured by EPMA are not this detailed. Consequently, for the purpose of comparison, the concentrations are spatially averaged and converted into a weight percentage with respect to the total UO_2 -Xe system as in standard EPMA measurements.

3. Results

3.1. Nominal parameter values

The 'nominal parameter set' (or equivalently the 'base case') used for the model parameters are listed in Table 1 along with the corresponding range of values found in open literature. Some of the nominal parameter values correspond to specific characterisations of the high burnup structure, e.g. grain size and pore separation, and as such have been

Table 1

Nominal parameter values (corresponding to an averaged xenon concentration of 0.16 wt%), along with parameter limits from the open literature and the corresponding impact on gas concentrations

Parameter	Nominal value	Parameter limits from open literature	Corresponding xenon concentration range/wt%
Grain diffusion coefficient, D_{grain}	$5.3 \times 10^{-22} \text{ m}^2 \text{ s}^{-1}$	10^{-24} – $10^{-20} \text{ m}^2 \text{ s}^{-1}$	46.1 – 6.7×10^{-3}
Bubble number density, N_{bl}	10^{12} m^{-2}	10^{11} – 10^{13} m^{-2}	0.16–0.54
Reference resolution rate coefficient, Γ_r	$2 \times 10^{-6} \text{ s}^{-1}$	10^{-7} – 10^{-4} s^{-1}	0.16–2.1
Grain boundary diffusion coefficient, D_{gb}	$2.6 \times 10^{-17} \text{ m}^2 \text{ s}^{-1}$	5.3×10^{-19} – $5.3 \times 10^{-16} \text{ m}^2 \text{ s}^{-1}$	2.1–0.13
Pore separation	3.0 μm	1.2–4.2 μm	0.13–0.20
Grain radius, R_{grain}	0.15 μm	0.05–0.3 μm	0.017–0.73
Pellet average fission rate density, \dot{F}	$6 \times 10^{18} \text{ m}^{-3} \text{ s}^{-1}$	10^{18} – $10^{19} \text{ m}^{-3} \text{ s}^{-1}$	0.057–0.23
Power peaking factor	3	1–4	0.085–0.20
Initial bubble radius of curvature, ρ_b	2 nm	1–10 nm	0.16–0.17
Grain boundary width, δ_{gb}	0.5 nm	–	–
Resolution rate coefficient, Γ_r	$9.1 \times 10^{-6} \text{ s}^{-1}$	–	–
Trapping rate coefficient, Ω	$6.7 \times 10^{-7} \text{ s}^{-1}$	–	–
Stable Xe chain yield	20.4%	–	–

set with the appropriate values taken from literature [7–12]. However, there are other parameters which are not well known for the high burnup structure (e.g. nucleating bubble number density). In this case the values of the normal fuel structure are used. However for certain parameter values there is considerable uncertainty and consequently we set these parameters such that the calculated averaged xenon concentration is close to the measured EPMA concentration (≈ 0.2 wt%), while staying within the parameter ranges specified in the literature. For instance, while the volume diffusion coefficient has been measured with various methods, there is still considerable uncertainty in the data, particularly for typical temperatures found in the high burnup structure. Moreover, the variation amongst the most commonly used correlations is quite large: for example the Turnbull three-term diffusion coefficient [24] at a temperature of 673 K and mass rating of 25 W/gU is $\approx 10^{-21} \text{ m}^2 \text{ s}^{-1}$, whilst the correlation derived by Matzke [25] gives $\approx 10^{-25} \text{ m}^2 \text{ s}^{-1}$. Furthermore, the volume diffusion coefficient correlations were derived from data for low to intermediate burnups and whilst they include irradiation enhancement they are not necessarily appropriate for higher burnups. Recent work by Hiernaut and Ronchi [26] indicates that the volume diffusion coefficient has an enthalpy that decreases with increasing burnup. However this work was performed under annealing conditions and may not apply to the steady state behaviour of high burnup fuel.

Another point to note is that for this model to achieve the ≈ 0.2 wt% Xe concentration the volume

diffusion coefficient needs to be reduced by a factor of 10 in comparison with the correlation. This is most likely due to the effect of the immobile intra-granular bubbles within the matrix that attenuates the diffusion coefficient [19], which is not directly accounted for in this model. Brémier and Walker [14] came to a similar conclusion in the Booth sphere calculation they performed to predict the observed high burnup structure xenon depletion of 0.2–0.3 wt%.

3.2. Sensitivity to parameter limits

As an initial assessment of the impact of the large uncertainties in the model parameters, the values of the averaged xenon concentration at the open-literature parameter limits have been calculated and are shown in the last column of Table 1. The calculations were performed by setting the parameter of interest to the upper and lower limits while retaining the nominal values for the remaining parameters.

It is clear from Table 1 that the volume diffusion coefficient has the largest effect on the averaged xenon concentrations with ~ 4 orders of magnitude variation for a volume diffusion coefficient range of 10^{-24} – $10^{-20} \text{ m}^2 \text{ s}^{-1}$. With such a large variation in concentrations the accuracy of measurements for the volume diffusion coefficient at low temperatures is clearly important. However we should note that a value of ~ 46 wt% is physically unrealistic as it is stating that the concentration of gas is approximately half of the UO_2 -Xe compound by weight. This is most unlikely to occur and clearly indicates the invalidity of this specific parameter combination.

It is interesting to observe that the average xenon concentration is relatively insensitive to variations of the HBS geometrical parameters, i.e. pore separation and grain radius. For the grain radius there is an increase in concentration with grain size, which might be of some concern given that the measured xenon concentration in the HBS zone is generally found to be constant. However, it should be noted that a grain radius distribution develops in the HBS zone [11] and thus the upper and lower limits should contribute less to the average concentration than the average grain radius of $0.15\ \mu\text{m}$. To confirm this, a simple Monte Carlo calculation was performed to reproduce the experimentally observed high burnup structure grain distribution. The introduction of a grain distribution was found to change the averaged xenon concentration by less than twice the nominal value.

Another point of remark is the variation of the averaged xenon concentration with the pellet averaged fission rate density. The selected range of $10^{18}\text{--}10^{19}\ \text{m}^{-3}\ \text{s}^{-1}$ corresponds approximately to pellet average linear heat rates of $2\ \text{kW/m}$ and $17\ \text{kW/m}$, respectively. The variation over this range is relatively small, i.e. less than an order of magnitude. More importantly, one would expect to have average linear heat rates of at least $10\ \text{kW/m}$ at steady state, which reduces this range even further.

Although the model assumes that bubble growth kinetics are not an important factor for the averaged xenon concentration the sensitivity with respect to the initial bubble radius was investigated. Typically, a nucleating bubble is expected to have a radius on the order of nanometers. As can be seen from Table 1, varying the initial bubble radius from 1 to 10 nm, even when considering bubble growth, does not significantly affect the averaged xenon concentration.

3.3. Sensitivity from two-parameter variations

The sensitivity of the averaged xenon concentration has been examined in greater detail for three parameters: (1) the grain boundary diffusion coefficient, (2) the resolution rate coefficient and (3) the bubble number density. To examine the effect of these parameters, several two-parameter variations were performed with the remaining model parameters fixed at their nominal values in each case.

Fig. 1 shows the effects of the variation of both the grain boundary diffusion coefficient and the bubble number density. The averaged xenon concentration saturates for high values of the grain boundary diffusion coefficient, for values greater than $\sim 10^{-17}\ \text{m}^2\ \text{s}^{-1}$ (greater than about 10^4 in the diffusion coefficient ratio), since the effective diffusion distance increases with the grain boundary

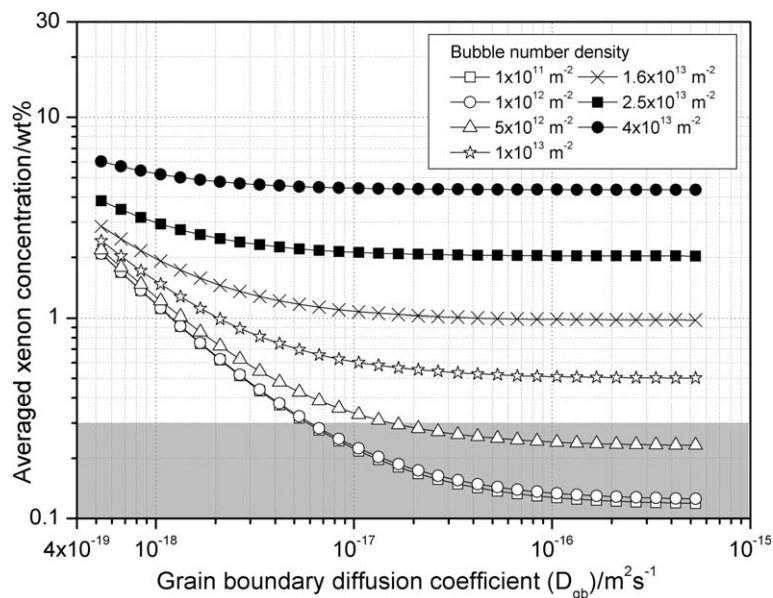


Fig. 1. Variation of the averaged xenon concentration with the grain boundary diffusion coefficient for different bubble number density values. The grey area corresponds to the range of average concentrations seen in EPMA measurements of the high burnup structure.

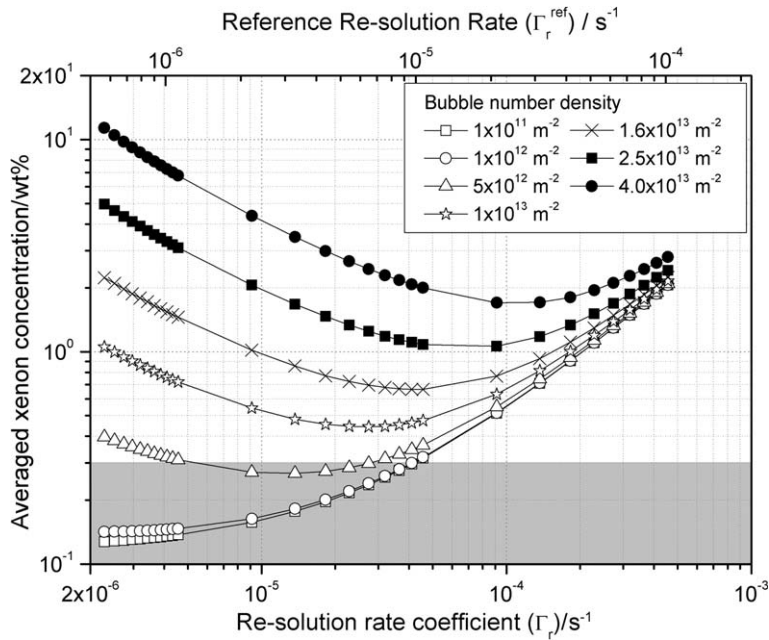


Fig. 2. Variation of the averaged xenon concentration with the resolution rate. The grey area corresponds to the range of average concentrations seen in EPMA measurements of the high burnup structure.

diffusion coefficient until the diffusion length is greater than the typical pore separation. In this regime, gas transport to the high-burnup pores is limited only by trapping. Therefore, a large sensitivity to the bubble number density is observed (if the bubble number density is increased from 10^{11} to $4 \times 10^{13} \text{ m}^{-2}$ then the averaged xenon concentration markedly increases from ~ 0.1 to $\sim 6 \text{ wt}\%$). When the bubble density is reduced below $\sim 10^{12} \text{ m}^{-2}$ there is an additional saturation effect due to a reduction in trapping strength yielding a large effective diffusion distance at the grain boundary. At lower diffusion coefficients, i.e. as the grain boundary diffusion coefficient approaches the volume diffusion coefficient, there is an expected considerable increase in the averaged xenon concentration as the grain boundary gas transport to the pores is greatly slowed down. It should be commented though that the saturation concentration, i.e. for a diffusion coefficient ratio above $\sim 10^4$, is dependent on the absolute value of the volume diffusion coefficient. From Fig. 1 we conclude that for the current model to achieve the $\sim 0.2 \text{ wt}\%$ averaged xenon concentration, the nucleating bubble number density needs to be low and the grain boundary diffusion coefficient should be high ($>10^4$ times the nominal volume diffusion coefficient).

Fig. 2 shows the dependence on both the resolution rate and the bubble number density. This plot illustrates two different regimes with respect to the resolution rate. At high resolution rates the concentration exhibits little variation with bubble number density and an upward trend while the opposite behaviour is observed at low resolution rates (bubble number density dependence and a downward trend with increasing resolution coefficient).

At high resolution rates the free gas available at the grain boundary is resolved immediately back into the grains, thus limiting the amount of gas diffusing out of the system via the grain boundary. This resolution flux acts as an additional source for the grains, which increases with the value of the resolution coefficient, yielding the observed upward trend. Moreover, as little free gas is available for trapping, the effect of the grain boundary bubbles is negligible in this regime.

However, at low resolution rates most of the free gas either leaves the system by grain boundary diffusion or is trapped in the bubbles. The resolution from the grain boundary bubbles is thus dominant in this regime and contributes moving part of this ‘immobile’ gas back into the grains thus allowing the possibility for further gas escape from the system via grain boundary diffusion. Therefore, in this regime

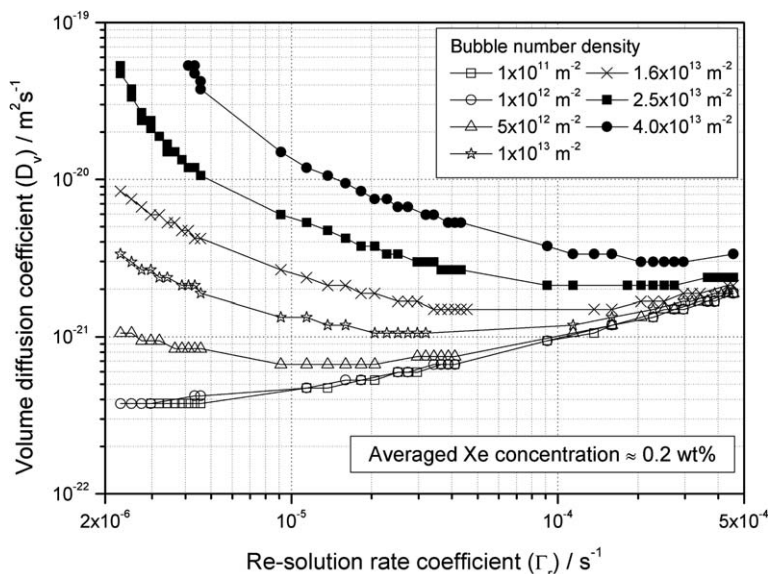


Fig. 3. Required range of values of volume diffusion coefficient, resolution rate coefficient and bubble number density for producing an ≈ 0.2 wt% averaged xenon concentration (diffusion coefficient ratio fixed at 5×10^4).

the average xenon concentration shows a downward trend with increasing resolution rate and a marked dependence on the bubble number density (the higher the bubble number density the more gas is trapped, thus remaining in the system).

Because of the multi-variable nature of the current model, different parameter combinations will lead to different averaged concentrations. Fig. 3 illustrates the range of values of the volume diffusion coefficient, resolution rate coefficient and bubble number density, over which the model produces an averaged xenon concentration of ~ 0.2 wt%. In this figure the diffusion coefficient ratio has been placed in the saturation regime, i.e. $\alpha = 5 \times 10^4$.

As expected, Fig. 3 exhibits most of the features that have been commented on previously, i.e.

- There is a lower sensitivity to the bubble number density at high resolution rates; this however develops strongly when the resolution rate is reduced.
- The range of the required volume diffusion coefficient (for attaining ~ 0.2 wt%) is well within the anticipated uncertainty on parameter values. However, it does mean that an accurate determination of diffusion coefficients is desirable for models of gas dynamics in the high burnup fuel.

4. Conclusions

A steady-state fission gas model has been developed to examine the gas dynamics in the high burnup structure. A stable solution was achieved for the set of parameters adopted in other fission gas models combined with parameter values specific to the HBS. With the current model it is possible to reproduce the 0.2 wt% experimentally observed xenon concentration under certain conditions, viz. fast grain boundary diffusion and a reduced volume diffusion coefficient. Our study has shown that the amount of gas staying in the system depends on the grain boundary diffusion coefficient only when the diffusivity ratio, α , is small, becoming otherwise insensitive to this quantity when $\alpha \geq 10^4$. Within the grain boundary diffusion saturation regime the current model exhibits a high sensitivity to three parameters: the volume diffusion coefficient, the bubble number density and the resolution rate coefficient. A more detailed examination of the sensitivity with respect to these parameters has shown that

1. The volume diffusion coefficient significantly affects the averaged xenon concentration and as such needs to be specified with a reasonable degree of accuracy.
2. The bubble number density is only of relevance to the averaged xenon concentration for densities

above 10^{12} m^{-2} and for resolution rate coefficients lower than $\sim 10^{-4} \text{ s}^{-1}$.

All of these observations are seen in Fig. 3, which illustrates the range of necessary combinations of these parameters for the 0.2 wt% concentration. From this 'locus' plot we infer that at low resolution rates all these three parameters are of relevance; however at higher resolution rates the bubble number density ceases to be an important factor and it is only the volume diffusion coefficient and the resolution rate coefficient that need to be specified. Of particular significance is the relatively small range of required values for the volume diffusion coefficient, which makes more accurate measurements of this quantity and the grain boundary diffusion coefficient highly desirable at low temperatures.

Further development of the current model into a time dependent description of the HBS gas evolution featuring additional mechanisms such as vacancy diffusion, bubble coarsening and effects of local stress fields is on-going.

Acknowledgements

The discussions with P. Van Uffelen, J. Spino (ITU) and M. Horvath (PSI) are gratefully acknowledged. The authors would also like to thank the Swiss nuclear utilities (*swissnuclear*) for financial support of the fuel research work at PSI.

References

- [1] J.R. Secker, B.J. Johansen, D.L. Stucker, O. Ozer, K. Ivanov, S. Yilmaz, E.H. Young, Nucl. Technol. 151 (2005) 109.
- [2] F. Schmitz, J. Papin, J. Nucl. Mater. 270 (1999) 55.
- [3] T. Fuketa, H. Sasajima, Y. Mori, K. Ishijima, J. Nucl. Mater. 248 (1997) 249.
- [4] High Burnup Effects Programme Final Report, DOE/NE/34046-1.
- [5] K. Lassmann, C.T. Walker, van de Laar, F. Lindström, J. Nucl. Mater. 226 (1995) 1.
- [6] IAEA, Fuel modeling at extended burnup, IAEA-TECDOC-998, Vienna, Austria, January 1998.
- [7] J. Spino, D. Papaioannou, J.P. Glatz, J. Nucl. Mater. 328 (2004) 67.
- [8] R. Manzel, C.T. Walker, J. Nucl. Mater. 301 (2002) 170.
- [9] J. Spino, D. Papaioannou, J. Nucl. Mater. 281 (2000) 146.
- [10] N. Lozano, L. Desgranges, D. Aymes, J.C. Niepce, J. Nucl. Mater. 257 (1998) 78.
- [11] J. Spino, K. Vennix, M. Coquerelle, J. Nucl. Mater. 231 (1996) 179.
- [12] T. Sonoda, M. Kinoshita, I.L.F. Ray, T. Wiss, H. Thiele, D. Pellottiero, V.V. Rondinella, H.J. Matzke, Nucl. Instrum. and Meth. B. 191 (2002) 622.
- [13] J. Noiro, L. Desgranges, P. Marimbeau, in: Proceedings of the International Seminar on Fission Gas Behaviour in Water Reactor Fuels, Cadarache France, Les Journees de Cadarache, 26–29 September 2000.
- [14] S. Brémier, C.T. Walker, Radiat. Eff. Def. S. 157 (2002) 311.
- [15] P. Losonen, J. Nucl. Mater. 304 (2002) 29.
- [16] H. Wallin, L.Å. Nordström, Ch. Hellwig, in: Proceedings of the International Seminar on Fission Gas Behaviour in Water Reactor Fuels, Cadarache France, Les Journees de Cadarache, 26–29 September 2000.
- [17] T. Kogai, J. Nucl. Mater. 244 (1997) 131.
- [18] M.S. Veshchunov, J. Nucl. Mater. 277 (2000) 67.
- [19] M.V. Speight, Nucl. Sci. Eng. 37 (1969) 180.
- [20] D.R. Olander, P. Van Uffelen, J. Nucl. Mater. 288 (2001) 137.
- [21] J. Rest, J. Nucl. Mater. 321 (2003) 305.
- [22] P. Van Uffelen, Contribution to the Modelling of Fission Gas Release in Light Water Reactor Fuel, Ph.D. Thesis, l'Université de Liège, SCK-CEN, January 2002.
- [23] Y. Kim, J. Nucl. Mater. 326 (2004) 97.
- [24] J.A. Turnbull, R.J. White, C. Wise, in: IAEA Technical Committee meeting on Water Reactor Fuel Element Computer Modelling in Steady-state, Transient and Accident Conditions, T1-TC-659, Preston, England, 1998, p. 168.
- [25] H.J. Matzke, Radiat. Eff. Def. S. 53 (1980) 219.
- [26] J.P. Hiernaut, C. Ronchi, J. Nucl. Mater. 294 (2001) 39.